

Effect of Ternary Scandium and Quaternary Zirconium and Titanium Additions on the Tensile and Precipitation Properties of Binary Cast Al-6Mg Alloys

M.S. Kaiser^{a*} and M.K. Banerjee^b

^a Bangladesh University of Engineering and Technology, Dhaka-1000, Bangladesh

^b National Institute of Foundry and Forge Technology, Ranchi 834003, India

Abstract

Effect of ageing on the mechanical properties of Al-6Mg alloy doped with 0.4 wt% scandium and with or without trace zirconium and titanium is studied. As cast, samples were aged isochronally for 60 minutes at different temperatures up to 500°C. The evaluation of tensile properties of the aged Al-6Mg (Sc, Zr, Ti) alloys was conducted by employing an Instron testing machine. Various strain rate of the tensile testing were used to find out the values of strain rate sensitivity of the experimental alloys. The influence of scandium is more pronounced on yield strength than on the tensile strength. Alloys with scandium, zirconium and titanium content have shown higher yield strength and the values of 'm' at peak-aged condition has been found to be comparatively high at quaternary addition. The fracture of the experimental alloys occurs through micro void coalescence. The transmission electron micrograph is seen to contain second phase constituent at the grain boundaries.

© 2008 Jordan Journal of Mechanical and Industrial Engineering. All rights reserved

Keywords: Al-Mg alloys; precipitates; strain hardening exponent; strain rate sensitivity; micro void;

1. Introduction

Aluminium-magnesium alloys are potential candidates for structural applications because of their low density, good weld ability, and excellent corrosion resistance [1]. Scandium is the most effective hardening element in aluminium alloy systems on an equal atomic basis to all other particle-forming elements alloyed with aluminium [2]. Addition of scandium has been shown to increase the strength while maintaining the ductility of aluminium-magnesium alloys [2, 3]. Scandium and zirconium to Al-Mg alloys synergistically promote strengthening and result in higher strengths than either Sc or Zr additions produce alone [4]. In Al-Mg-Sc alloys with Zr additions, strengthening occurs primarily by development of coherent Al₃Sc and Al₃Zr dispersions. Additional strengthening is achieved by grain refinement, as the dispersions inhibit recrystallization during working [4].

In view of the fact that zirconium and titanium form their individual aluminides, the quaternary addition of Zr or Ti to Al-Mg-Sc alloy must have some bearing on the structure and mechanical properties of the cast alloys. Since fracture toughness of most aluminium alloys are determined by the nature of second phase particles present

in the microstructure of the alloy along with its grain structure, it appears that the precipitates due to scandium should appreciably influence the fracture toughness behaviour of the cast alloys [5, 6].

The moderate strength level achieved in Al-Mg-Sc alloys combined with the inherent corrosion resistance of the Al-Mg system makes these alloys attractive for airframe structural applications. Sc-bearing dispersoids are inherently thermally stable [7], which enable consideration for structural applications where extended elevated temperatures are anticipated. However, in alloys with magnesium levels above about 3.5%, precipitation of the β phase, Al₃Mg₅, can occur during thermal exposure and are detrimental to corrosion resistance [7].

It is the purpose of the current investigation to understand the influence of scandium as a minor additive on the mechanical properties of Al-6Mg-Sc alloy system. This work is intended to determine if alloys of this type could be competitive with other low-density systems for high performance applications. Zirconium and titanium form their aluminides and are influential to the precipitation behaviour of Al₃Sc in Al-Mg alloys. Therefore, to study the achievable properties of Al-6wt% Mg-0.4wt% Sc alloy with quaternary additions of zirconium and titanium is significant. The ability of Al₃Sc precipitates to stabilise substructure envisages the use of

* Corresponding author. e-mail: mskaiser@iat.buet.ac.bd

strain hardening for enhancement of mechanical properties of the alloy. Since strain-hardening behaviour of alloys is sensitive to strain rate of testing, the study on the tensile properties of the alloys under various thermal and mechanical treatment has been carried out for various strain rates of testing. Due to fine distribution of Al_3Sc , previous workers [2, 8] have studied particles super plastic effect in Al-Mg-Sc alloy. Super plasticity in metals and alloys are characterized by strain rate sensitivity values. The variations of strain rate sensitivity of the experimental alloys after thermal treatments are also studied in order to reach a conclusion about the possible deformation mode operative in the experimental alloys.

2. Experimental Methods

Four alloys were produced by melting in a resistance heating pot furnace under the suitable flux cover (degasser, borax . . . etc.). Several heats were taken for developing base Aluminium-Magnesium alloy, Aluminium-Magnesium alloy containing scandium and with or without zirconium and titanium. First, the aluminium (99.5% purity) and aluminium-scandium master alloy (2%Sc) were melted in a clay-graphite crucible, and then magnesium ribbon (99.7% purity) was added by dipping into the molten metal. Zirconium and titanium were taken in the form of powder (99.98% purity) with in a cover of aluminium foil and were then added by plunging. The final temperature of the melt was always maintained at $780 \pm 15^\circ C$ with the help of the electronic controller. Then the melt was homogenised under stirring at $700^\circ C$. Casting was done in cast iron metal moulds preheated to $200^\circ C$. Mould sizes were 12.5 x 51.0 x 200.0 in millimetre. All the alloys were analysed by wet chemical and spectrochemical methods simultaneously. The chemical compositions of the alloys are given in Table 1.

The cast alloys were cut to pieces of suitable size 10mm x 10mm x 10mm and were subjected to isochronal ageing treatment for 60 minutes at different temperature up to $500^\circ C$. The aged alloys were then put to Vickers hardness testing at 5 kg load for assessing the age hardening effect of the alloys. An average of ten concordant reading has been taken as the representative hardness of a sample. Tensile testing of aged samples was carried out in an Instron testing machine of model no. 4204, using different crosshead speed to maintain the strain rate of $10^{-2} s^{-1}$, $10^{-3} s^{-1}$, and $10^{-4} s^{-1}$. The samples used were according to ASTM specification. Fractograph observations of the surfaces fractured by tensile testing

were also carried out in a Joel Scanning Electron Microscope type JSM-5200 at various magnifications. Before fractography, the samples were cleaned by alcohol. Transmission Electron Microscopic studies of alloys in aged and thermo mechanically treated condition were carried out in Philips (CM12) make Transmission Microscope at 160 KV. The samples were thinned in a jet of nitric acid and ethyl alcohol (3:7) at 263 K as electrolyte. The observations were carried out with sample tilts wherever needed.

3. Results

3.1. Isochronal Ageing

The results of isochronal ageing of all the four alloys are shown in Fig. 1. It is seen that all the alloys except binary alloy (alloy 1) have shown appreciable ageing response. Alloy 1 has however shown a continuous softening at increasing ageing temperatures, with a steeper hardness drop beyond $400^\circ C$. In all cases, the peak hardness is obtained at around $300^\circ C$. When zirconium is added to the alloy containing 0.4 wt% scandium (alloy 3), both the extent of age hardening and the peak hardness value are seen to increase quite considerably. However, the temperature at which peak hardness is attained remains essentially the same. In alloy 4 titanium are added to the alloy in place of zirconium. Its peak ageing hardness is seemingly higher than the others are. Beyond peak hardness, value the usual softening due to annealing takes place. Alloy 2 with 0.4 wt% Sc possesses maximum resistance to age softening. Zirconium bearing alloy shows the maximum softening rate within a temperature range of $300^\circ C$ - $400^\circ C$.

3.2. Tensile properties

The results of tensile tests of the alloys under various preparation parameters are tabulated in Table 2. The variation of ultimate tensile strength, yield strength and percentage elongation under various ageing conditions of the alloys 1 to 4 are shown in Figs. 2-4. The test values obtained at a strain rate of testing $10^{-3} s^{-1}$ are used to plot the graphs. It is seen from Fig. 2 that the scandium doped alloys experience extra strengthening due to age hardening effect and the maximum in tensile strength value are achieved at an ageing temperature of $300^\circ C$.

Table 1. Chemical Composition of the Experimental Alloys (wt %)

Alloy	Mg	Sc	Zr	Ti	Cu	Fe	Mn	Ni	Si	Zn	Cr	Sn	Al
1	6.10	0.000	0.000	0.001	0.081	0.382	0.155	0.003	0.380	0.136	0.002	0.002	Bal
2	5.97	0.400	0.000	0.002	0.071	0.314	0.107	0.002	0.335	0.124	0.002	0.002	Bal
3	5.85	0.400	0.185	0.003	0.069	0.335	0.112	0.001	0.345	0.170	0.003	0.002	Bal
4	6.06	0.400	0.000	0.175	0.080	0.306	0.104	0.002	0.335	0.170	0.002	0.002	Bal
Remarks:	Alloy 1	Al -6 wt % Mg											
	Alloy 2	Al -6 wt % Mg -0.4 wt % Sc											
	Alloy 3	Al -6 wt % Mg -0.4 wt % Sc -0.2 wt % Zr											
	Alloy 4	Al -6 wt % Mg -0.4 wt % Sc -0.2 wt % Ti											

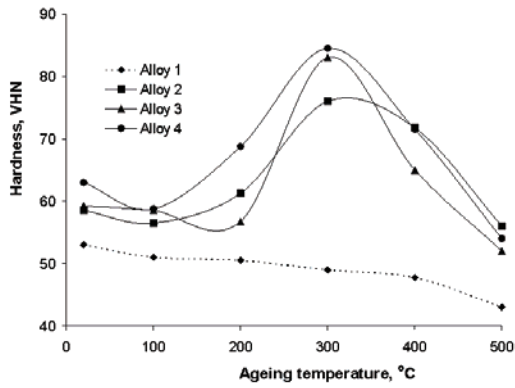


Fig. 1: Isochronal ageing curve of the cast alloys aged for 1 hour.

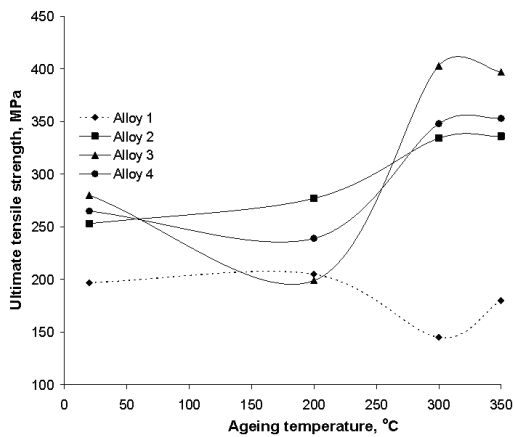


Fig. 2: Variation of ultimate tensile strength (10^3 s^{-1}) with ageing temperature of cast alloys isochronally aged for 1 hour.

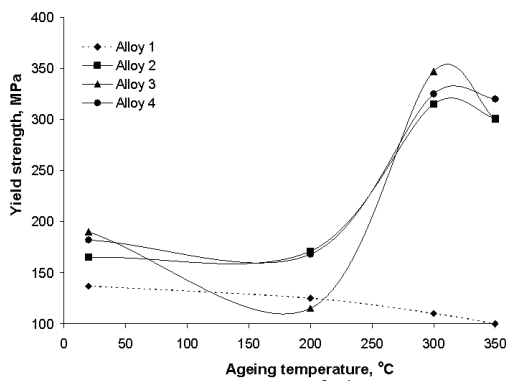


Fig. 3: Variation of yield strength (10^3 s^{-1}) with ageing temperature of cast alloys isochronally aged for 1 hour.

From the nature of variation in yield strength with ageing temperature of the cast alloys (Fig. 3), it appears that the yield strength of the scandium added alloys increase to peak value at an ageing temperature of 300°C. Beyond 300°C, further ageing has lowered the yield strength of the alloys. The base alloy does not show any variation in yield strength with ageing temperature. It is clearly visible from Figs. 2 and 3 that additions of zirconium and titanium have enhanced the strength properties due to precipitation hardening when aged at 300°C. However, for both the alloys (alloys 3 and 4) a marginal decrease in tensile strength is observed during the initial period of ageing. However, this trend is not prominent in alloy 4 in the case of yield strength (Fig. 3).

Interestingly the yield strength is found not influenced by quaternary additions of zirconium or titanium. On the contrary, quaternary additions have led to significant improvement in ductility after being aged at 300°C and above (Fig. 4).

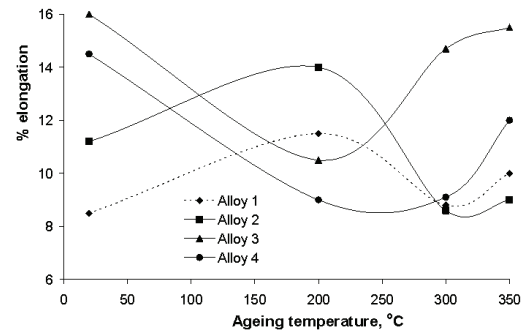


Fig. 4: Variation of percent elongation (10^3 s^{-1}) with ageing temperature of cast alloys isochronally aged for 1 hour.

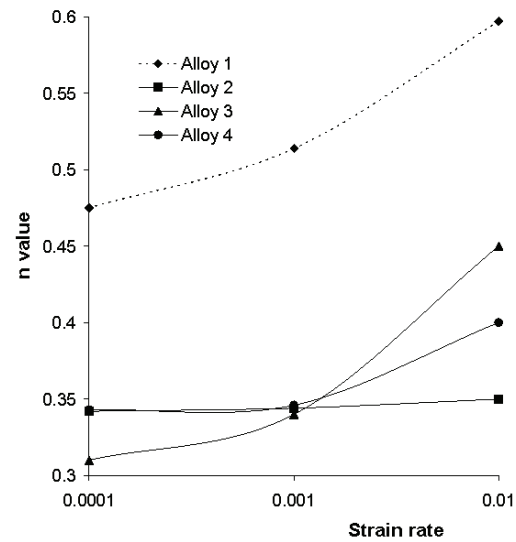


Fig. 5: Variation of strain hardening exponent with strain rate of testing of cast alloys aged at 300°C.

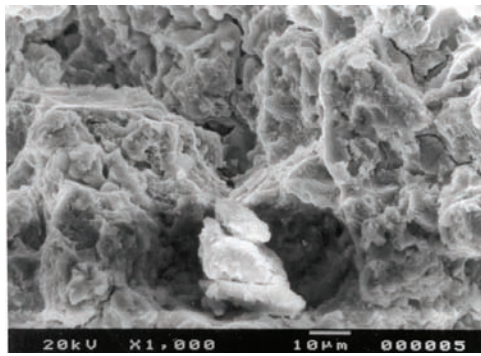
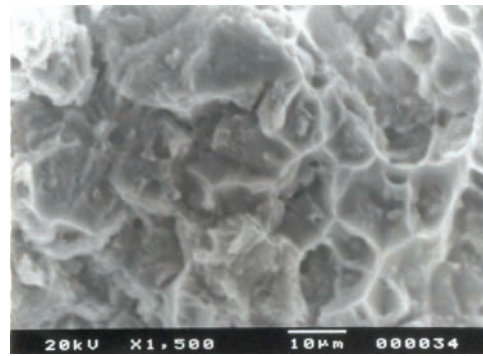
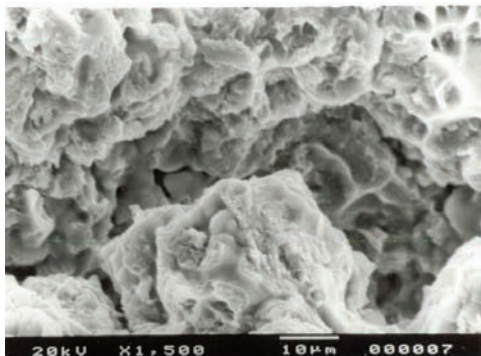
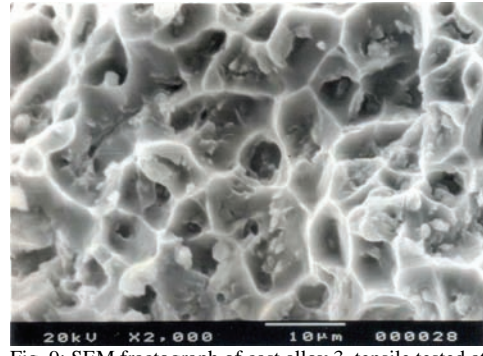
From Table 2, it appears that increasing strain rate has increased the tensile and yield strength of the experimental alloys. It is further observed that the change in strength properties is found to be less (~ 30 MPa) in case alloys 2-4 aged at 300°C. It is seen that the strain hardening exponent 'n' of the experimental alloys range from 0.310 to 0.597 after ageing at 300°C (Fig. 5). For alloys with minor additions (alloys 2-4), the strain hardening exponent values lie between 0.310 and 0.450. From Table 2 it is found that the strain rate sensitivity (m) of the experimental alloys lies within 0.05-0.07 and m values are higher for scandium added alloys.

3.3. Fractography

The fractography studies of the cast and aged alloy 2, tensile tested at different strain rates (Figs. 6-8) show evidences of microvoid coalescence. The cast alloy three, with quaternary addition shows fracture due to creation of voids (Fig. 9). Fracture surface of both alloys exhibited fine dimples indicating ductile rupture.

Table 2: Tensile Properties Of The Cast Alloys

Alloy no.	History	Strain Rate (s^{-1})	Tensile Properties			n Value	m Value
			UTS (MPa)	YS (MPa)	Elongation (%)		
1	As cast	10^{-3}	197	137	8.5	-	-
	As cast /aged at 200°C	10^{-3}	205	125	11.5		
	As cast /aged at 300°C	10^{-2}	180	130	8.8	0.597	0.049
		10^{-3}	145	110	8.8	0.514	
		10^{-4}	127	100	9.2	0.475	
As cast /aged at 350°C	10^{-3}	180	100	10			
2	As cast	10^{-3}	253	165	11.2		
	As cast /aged at 200°C	10^{-3}	277	171	14.0		
	As cast /aged at 300°C	10^{-2}	338	325	8.3	0.350	0.058
		10^{-3}	334	315	8.6	0.344	
		10^{-4}	329	303	10.0	0.342	
As cast /aged at 350°C	10^{-3}	336	301	9.00			
3	As cast	10^{-3}	280	190	16.0		
	As cast /aged at 200°C	10^{-3}	199	115	10.5		
	As cast /aged at 300°C	10^{-2}	408	380	13.8	0.450	0.055
		10^{-3}	403	347	14.7	0.340	
		10^{-4}	392	340	14.8	0.310	
As cast /aged at 350°C	10^{-3}	397	300	15.5			
4	As cast	10^{-3}	265	182	14.5		
	As cast /aged at 200°C	10^{-3}	239	168	9.0		
	As cast /aged at 300°C	10^{-2}	375	337	8.3	0.400	0.049
		10^{-3}	348	325	9.1	0.346	
		10^{-4}	325	304	10.4	0.343	
As cast /aged at 350°C	10^{-3}	353	320	12.0			

Fig. 6: SEM fractograph of cast alloy 2, aged at 300°C for 1 hour and tensile tested at strain rate of $10^{-3}s^{-1}$.Fig. 8: SEM fractograph of cast alloy 2, aged at 300°C for 1 hour and tensile tested at strain rate of $10^{-2}s^{-1}$.Fig. 7: SEM fractograph of cast alloy 2, aged at 300°C for 1 hour and tensile tested at strain rate of $10^{-3}s^{-1}$.Fig. 9: SEM fractograph of cast alloy 3, tensile tested at strain rate of $10^{-3}s^{-1}$.

3.4. Transmission electron microscopy

The transmission electron micrograph of alloy 3, cast and annealed at 300°C is seen to contain second phase constituent at the grain boundaries (Fig. 10). The dark field image of one of the second phase particle is shown in Fig. 11. TEM image of the same alloy at a higher magnification shows irregular boundaries with high amount of precipitates (Fig. 12).

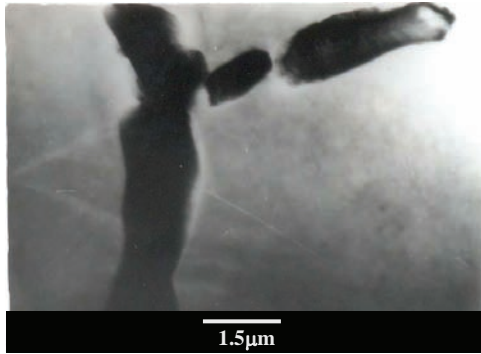


Fig. 10: TEM micrograph of cast alloy 3 aged at 300°C for 1 hour.

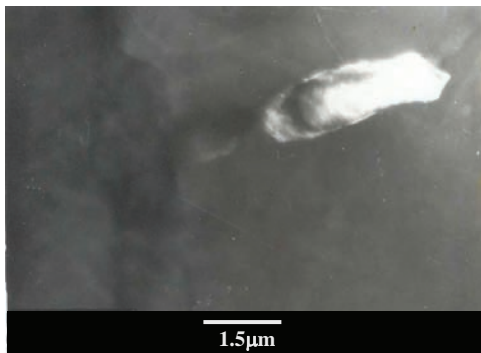


Fig. 11: TEM micrograph (dark field) of cast alloy 3 aged at 300°C for 1 hour.

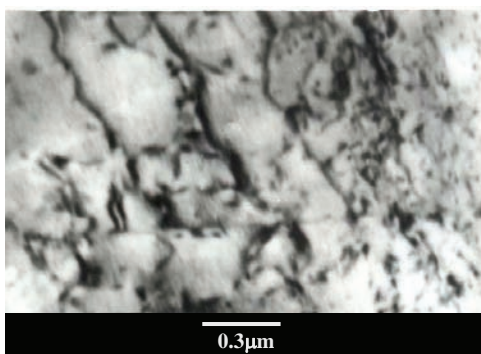


Fig. 12: TEM micrograph of cast alloy 3 aged at 300°C for 1 hour.

4. Discussions

The results of the present experiments clearly indicate that the age hardening effect shown by the alloys are purely due to addition of scandium. Scandium when added in small concentrations is known to refine the grain structure of cast metal and to form a supersaturated solid

solution upon solidification [3, 9]. Formation of supersaturated solid solution assures a high precipitation hardening effect upon decomposition of this solid solution with the formation of fine coherent equilibrium Al_3Sc precipitates [10-11]. No ageing response is visible for the base alloy. In the cast condition the β -phase being already present in the microstructure of the matrix of alloy 1, precipitation hardening due to the formation of aluminides of magnesium is not envisaged. Moreover Al-Mg alloys are known to be incapable of producing significant age hardening even though the binary phase diagram contains a sloping solvus [12, 13].

From the isochronal ageing curves, it is seen that Al_3Sc precipitates form most rapidly at around 300°C, where the peak-ageing hardness values are obtained. The softening of the alloys at higher temperature may be due to particle coarsening effect. The initial softening shown in the isochronal ageing curve (Fig. 1) is thought to be due to internal stress relieving of the rapidly solidified castings. Because the addition of scandium and zirconium/titanium in Al-Mg alloys leads to the formation of sufficient amount of dispersoids in the microstructure, alloys 3 and 4 give the highest age hardening effect.

From the results of Fig. 2, it is clear that strengthening due to ageing takes place to the maximum extent at the ageing temperature 300°C. Incidentally, maximum ageing hardness has occurred at this temperature. Thus, improvement in strength during ageing is due to the formation of Al_3Sc precipitates, which are known to have LI_2 crystal structure. The precipitates remain coherent at the peak ageing temperature. Fig. 3 clearly delineates that improvement in yield strength of the alloys due to ageing is more than that for ultimate strength. Thus with the progress of ageing yield tensile ratio increases. Material toughness is related to this ratio. It is known that yield strength is a structure sensitive property of the material and hence formation of fine precipitates is more responsive to yield strength. From the same figure one may observe that significant influence on yield strength is obtainable only for ageing temperatures 300°C or 350°C where an appreciable amount of Al_3Sc is formed. Until the time, the amount of Al_3Sc precipitates has not been perceptible in the microstructures, no variation in yield strength is practically noticed (200°C ageing). Again, the influence of scandium is much pronounced on yield strength than on the tensile strength due to the already stated reasons that fine coherent precipitates of Al_3Sc are responsive much more to the yield behaviour of the alloys. Hence higher volume fraction of the precipitates in alloys with higher scandium content exerts greater influence on the yield strength. Earlier workers have observed such scandium dependence of yield strength of aluminium alloys too [14]. Mechanism of precipitation strengthening has been elaborately reviewed earlier [five]. In general, small coherent particles prohibit the movement of dislocations; as a result strength rises until the particle size becomes so large that the Orvan bypassing mechanism comes into operation. Contribution to the strength of the precipitation-hardened alloy comes mainly from the elastic coherency strains at particle/matrix interface but appreciable contribution to strength would also come from the work for creating anti-phase domain boundary in the event the moving dislocations cut through the ordered coherent

precipitate. In the present case, Al_3Sc is coherent and ordered. Calculation have shown that combining the contributions from coherency and order hardening gives an overall increase in strength due to Al_3Sc of a magnitude close to what could be observed experimentally [15]. Therefore the existing theories of strengthening of materials by coherent, ordered precipitate account for the observed variation of strength properties of the alloys in the present experiments.

The occurrence of ductility minima at the peak-aged condition is easily understandable since the inhomogeneous deformation due to dislocation movement being operative during tensile loading would always lead to a lowering of toughness. In fact, the fine precipitates of Al_3Sc act as the early nucleation sites for micro voids. Therefore, fracture resistance of the material decreases. This is reflected in the form of minimum percent elongation of the alloys aged at 300°C whence the density of fine precipitates is the maximum. In the alloys with quaternary additions, there is an improvement of peak UTS by 70 MPa with zirconium addition and 40 MPa with titanium addition. However, these quaternary additions have negligible effect on the yield strength of the alloys under peak-aged condition. Addition of zirconium and titanium leads to the formation of corresponding aluminides viz. Al_3Zr and Al_3Ti . These precipitate particles induce the formation of Al_3Sc . Thus although the volume fraction of precipitates is increased, there is no specific increment in the degree of dislocation cutting. This is because average precipitate size is increased to the level where the particles become strong enough to withstand being cut by dislocations. However, Orwan bypassing mechanism becomes the operational deformation mode. As a result, homogeneous deformation takes place and the toughness of the material improves. This is supported by the percentage elongation values of the alloys with quaternary additions, which is appreciably high for Zr-added alloy at the peak-aged condition.

It is known that tensile strength of alloys increases with increasing strain rate. It is also known that yield stress and flow stress at low plastic strains are more dependent on strain rate of testing than the tensile strength. In the present experiments it is recorded that both tensile and yield strength have increased with increasing strain rate. Thus, the experimental results are commensurate with the existing knowledge in this regard. In the present case the plastic strain is in general small and it assumes slightly higher value only after over ageing. Therefore, the results of the present experiments do not reveal any difference in the responsiveness of yield and tensile strength towards the strain rate of testing. The lower values of strain hardening exponent over that of the base alloy is attributed to the formation of Al_3Sc , which increases the yield stress. Therefore, extra hardening during post yielding plastic deformation is limited by its tensile strength, which is not far greater than the yield strength as substantiated by the high yield/tensile ratio of the alloys.

Velocity of mobile dislocations is linearly proportional to strain rate. Again, velocity of dislocations is strongly dependent on flow stress ($u = A\sigma^m$, where 'u' dislocation velocity, 'A' constant, ' σ ' mean true stress including the internal stress, and strain rate sensitivity, $m = 1/n'$). It may be deduced that for a specific strain increment an increase

in the velocity of mobile dislocations would lead to an increase in 'n' values as it increases the flow stress. Now increasing strain rate leads to an increase in the velocity of dislocations. This is why the 'n' values of the experimental alloys are seen to increase with increasing strain rate of testing. However, for alloy 2 the microstructure after ageing at 300°C contains maximum amount of fine precipitates of Al_3Sc . It is already demonstrated that this precipitate formation is not dislocation induced [6]. Hence, during tensile straining of materials with this type of microstructures, dislocation motion is greatly inhibited by the precipitate particles. Thus within the range of variation in strain rate of testing, the velocity of mobile dislocations cannot appreciably increase due to the inhibitions stated above. Therefore, 'n' value remains essentially independent of strain rate of testing (Fig. 5).

It is known that strain rate sensitivity of metals and alloys are rather low (< 0.1) at room temperature although it increases significantly above half the melting point. Scandium refines the grain size of Al-6Mg alloy and leads to the formation of coherent precipitates of Al_3Sc . As a result, scandium doped Al-6Mg alloy is micro structurally conducive to super plasticity at elevated temperature. In fact, super plastic behaviour is already reported in similar alloys [6, 16] where 'm' values were found range from 0.33-0.50 within a temperature span of 350°C – 475°C . In the present case, the room temperature values of 'm' are comparatively high and hint upon its inherent super plastic behaviour at elevated temperatures.

Fractography of alloy 2 cast and annealed at 300°C shows that micro voids coalescence is the chief mode of failure (Fig. 6). Numerous micro voids are also observed in Fig. 6. The characteristic dimples are observed in Fig. 7. Some kind of particles is observed to be present at the base of the dimples. Fracture might have been initiated by these particles. These particles are involved in creating micro voids is also noticed in the same fractograph (Fig. 8). This implies a ductile fracture. Testing at higher strain rate does not exhibit much difference in the character of fracture.

Alloy 3 tested at room temperature exhibits dimples characteristics of ductile failure. This means that this alloy is inherently ductile. Some particles presumably of Al_8Mg_5 are seen to be present at the base of dimples. These particles are rather fine and are promoted homogeneous deformation. However, it is seen from the fractograph in Fig. 9 that these particles are fractured to aid in creation of voids. Well-defined shear ridges beautifully characterize ductile shear.

The transmission electron micrograph of alloy 3 containing zirconium is seen to contain second phase constituent at the grain boundaries. At this resolution, the bright field image has not been able to bring the precipitates into full contrast. It just appears that very fine precipitates are present intragranularly. The dark field image of one of the second phase particle is shown in Fig. 11. The second phase constituents are supposed to be primarily Mg_5Al_8 . However, other aluminides of transition metals (present in traces in aluminium) along with Al_3Zr might have remained dissolved in them [16, 17].

The bright field image of the same alloy at a higher resolution shows irregular boundaries with a huge amount of intragranular precipitates. The deformation contrast around the precipitates is indicative of coherency of the

precipitates. The solidification strain has resulted into dislocations. A large number of precipitates are found to form at the dislocations as the strain field near them assist nucleation by reducing strain energy required to form a nucleus. However, the precipitates are seen to have grown coherently. However, the dislocation-induced precipitation in alloy 3 is to be explained based on the role played by zirconium in the process of nucleation of precipitates. Al_3Zr and Al_3Sc are both known to be of L1_2 crystal structure. They are known to be mutually soluble in each other and are isomorphism. Thus it is conjectured that Al_3Zr is formed first at dislocations in alloy three as it is already reported earlier that Al_3Zr precipitation is facilitated at dislocations [1, 18]. In order to decrease nucleation energy Al_3Zr particles are formed at dislocations already available in the cast alloy. These particles induce the formation of Al_3Sc , which is dissolved thereby to form precipitates of the type $\text{Al}_3(\text{Zr}_x\text{Sc}_{1-x})$. Whether the process of nucleation is inset or not remains nebulous at this stage. The precipitates are uniformly distributed within a size range of 15-20 nm with an average antiparticle distance of around 30 nm. The larger size of these precipitates seemingly indicates that there is separate formation of Al_3Zr first and subsequently the formation of Al_3Sc and its dissolution into Al_3Zr leads to the formation of $\text{Al}_3(\text{Zr}_x\text{Sc}_{1-x})$; the chance of direct nucleation of $\text{Al}_3(\text{Zr}_x\text{Sc}_{1-x})$ can not be concluded from the results of the present experiments.

5. Conclusions

1. Binary Al-6Mg alloy is not age hardenable. Minor addition of scandium leads to significant age hardening due to precipitation of coherent Al_3Sc precipitates.
2. The influence of scandium is much pronounced on yield strength than on the tensile strength, as fine coherent precipitates of Al_3Sc are much more responsive to the yield behaviour of the alloys. Scandium improves yield strength quite considerably. Quaternary addition of zirconium and titanium also increases both tensile and yield strength.
3. The room temperature values of 'm' are comparatively high and hints upon super plastic behaviour of the alloys at elevated temperatures. The fracture of the experimental alloys occurs through micro void coalescence.
4. Addition of zirconium ensures dislocation-aided precipitation of Al_3Zr , which induces the precipitation of Al_3Sc . This ultimately results in the formation of $\text{Al}_3\text{Zr}_x\text{Sc}_{1-x}$.

Acknowledgements

The authors gratefully acknowledge sponsorship by University Grants Commission, New Delhi, India.

References

- [1] J. E. Hatch, "Aluminium Properties and Physical Metallurgy" American Society for Metals, 1984, 236.
- [2] R. Sawtell and C. L. Jensen, "Mechanical properties and microstructures of Al-Mg-Sc alloys." Metallurgical Transactions A, Vol. 21, 1990, 421-430.
- [3] Yu. A. Filatov, V. I. Yelagin and V. V. Zakharov, "New Al-Mg-Sc alloys", Material Science and Engineering, Vol. A280, 2000, 97-101.
- [4] Z. Jie., Y. Zhimin, Z. Yonghong, G. Yongzheng, and P. Qinglin, "Microstructure of differently treated Al-Mg-Sc-Zr alloys." Journal of Central South University of Technology, Vol. 4, No. 1, 1997, 24-27.
- [5] S. Lee, A. Utsunomiya, H. Akamatsu, K. Neishi, N. Furukawa, Z. Horita and T.G. Langdon, "Influence of Scandium and Zirconium on Grain Stability and Super plastic Ductility's in Ultrafine-Grained Al-Mg Alloys". Acta Mater., Vol. 50, 2002, 553-564.
- [6] Toropova L. S., Eskin D. G., Kharakterova M. L. and Dobatkina T.V.: Advanced Aluminium Alloys Containing Scandium, Structure and Properties, Baikov Institute of Metallurgy, Moscow, Gordon and Breach Science Publishers, Russia, 1998.
- [7] R. Braun, B. Lenczowski and G. Tempus, "Effect of Thermal Exposure on the Corrosion Properties of an Al-Mg-Sc Alloy Sheet," Mater. Sci. Forum, Vol. 331-337, 2000, 1647-1652.
- [8] T. G. Nieh, R. Kaibyshev, L. M. Hsiung, N. Nguyen and J. Wadsworth, "Subgrain formation and evolution during the deformation of an Al-Mg-Sc alloy at elevated temperature", Scripta Mater., Vol. 36, No. 9, 1997, 1011-1016.
- [9] T. Aiura, N. Sugawara and Y. Miura, "The effect of scandium on the As-Homogenized Microstructure of 5083 Alloy for Extrusion," Materials Science and Engineering, Vol. 280, 2000, 139-145.
- [10] M. E. Drits, J. Dutkiewicz, L. S. Toropova and J. Salawa, "The effect of Solution Treatment on the Ageing Process of Al-Sc Alloys," Crystal Res. And Techno, No. 19, 1984, pp. 1325-1330.
- [11] M. E. Drits, L. S. Toropova, G. K. Anastas'eva and G. L. Nagornichnykh, "The effect of Homogenizing Heating on the Properties of Alloys in the Al-Sc and Al-Mg-Sc Systems", Russ. Metal., No. 3, 1984, 192-195.
- [12] Polmear IJ: Light Alloys, Metallurgy of the Light Metals, Edward Arnold (Publishers) Ltd 41 Bedford Square, London WC1B 3DQ 1981.
- [13] N. Bo, Y. Zhi-min, Z. Da-peng, P. Yong-yi, J. Feng and H. Ji-wu, "Effect of homogenization treatment on microstructure and properties of Al-Mg-Mn-Sc-Zr alloy", Journal of Central South University of Technology, Vol. 14, No. 4, 2007, 452-455.
- [14] T. Torma, E. Kovacs-Csetenyi, L. Vitalis, J. Stepanov and M. Butova, "The Effect of Scandium Addition on the Mechanical Properties of Pure Aluminium and of an AlMg6 Alloy." Material Science Forum, Vol. 13/14, 1987, 497-503.
- [15] B. A. Parker, Z. F. Zhou, and P. Nolle, "The Effect of Small Additions of Scandium on the Properties of Aluminium Alloys". Journal of Materials Science No. 30, 1995, 452-458.
- [16] J. Royset and N. Ryum, "Scandium in aluminium alloys." International Materials Reviews, Vol. 50, No. 1, 2005, 19-44
- [17] C. B. Fuller, D. N. Seidman, and D. C. Dunand, "Mechanical properties of Al (Sc, Zr) alloys at ambient and elevated temperatures". Acta Materialia, Vol. 51, 2003, 4803-4814.
- [18] K.L. Kendig and D.B. Miracle, "Strengthening mechanisms of an Al-Mg-Sc-Zr alloy." Acta Materialia Vol. 50, 2002, 4165-4175.

